SHEAR BUCKLING OF THIN-WALLED CHANNEL SECTIONS WITH COMPLEX STIFFENED WEBS

SONG HONG PHAM
CAO HUNG PHAM
GREGORY J. HANCOCK

RESEARCH REPORT R924
JANUARY 2012

ISSN 1833-2781

SCHOOL OF CIVIL ENGINEERING

THE UNIVERSITY OF SYDNEY

THE UNIVERSITY OF SYDNEY

SCHOOL OF CIVIL ENGINEERING

SHEAR BUCKLING OF THIN-WALLED CHANNEL SECTIONS WITH COMPLEX STIFFENED WEBS.

RESEARCH REPORT R924

SONG HONG PHAM
CAO HUNG PHAM
GREGORY J. HANCOCK

January 2012

ISSN 1833-2781

ISSN 1833-2781

Published by:
School of Civil Engineering
The University of Sydney
Sydney NSW 2006
Australia

This report and other Research Reports published by the School of Civil Engineering are available at http://sydney.edu.au/civil

ABSTRACT

For cold-formed channel section design in shear, the traditional approach has been to investigate shear plate buckling in the web alone. Recently, an improvement in the elastic buckling stress of the whole thin-walled channel section including flanges and lips in pure shear has been demonstrated. For webs with relatively large depth to thickness ratios, the local buckling mode in shear occurs mainly in web. The structural efficiency of such a web can be improved by adding intermediate stiffeners cold-formed longitudinally in the middle of the webs.

This report presents numerical buckling analyses implemented by means of the Semi-Analytical Finite Strip Method (SAFSM). The shear signature curve from the SAFSM is used in a design proposal for a newly developed Direct Strength Method (DSM) for shear. The DSM was formally adopted in the North American Design Specification in 2004 and in the Australian/New Zealand Standard for Cold-Formed Steel Structures (AS/NZS 4600:2005) in 2005 as an alternative to the traditional Effective Width Method (EWM). The theory and development of the shear signature curve has been clearly presented and discussed by Hancock and Pham (2011). The objective of this report is to apply this methodology to investigate the effect of web stiffeners on the elastic shear buckling stress by varying the number, shapes and locations of the longitudinal web stiffeners. A series of shear signature curves and corresponding buckling mode shapes are studied in three different cases of web stiffener geometry where the variables are stiffener position and dimensions. The results from the analysis are included to identify local and distortional buckling caused by shear stresses. The explanation of the occurrence or disappearance of the minima of the shear signature curves where local or distortional buckling occur is also discussed.

KEYWORDS

Cold-formed steel; Web stiffener; Elastic buckling; Complex channel sections; High strength steel; Direct strength method.

TABLE OF CONTENTS

INTRODUCTION

SEMI-ANALYTICAL FINITE STRIP METHOD (SAFSM) FOR SHEAR

SAFSM was originally derived by Cheung (1968) for stress analysis of simply supported isotropic and orthotropic plates in bending and firstly applied to the buckling analysis of plate assemblies under biaxial compression by Przmieniecki (1973). This method was further extended by Plank and Wittrick (1974) to analyse the buckling behaviour of thin-walled cross-sections under the various loading conditions such as longitudinal and transverse compression, longitudinal in-plane bending and shear. Hancock (1978) applied the SAFSM to beams and identified local, distortional and lateral-torsional modes. The signature curve for a beam being the buckling stress versus the buckling half-wavelength for a single half-wavelength was also identified by Hancock (1978). However, the application of the SAFSM for pure shear buckling analysis has not been studied.

Pham and Hancock employed the Spline Finite Strip Method (SFSM) developed by Lau and Hancock (1986) to study the elastic buckling of thin-walled channel sections (Pham and Hancock, 2009a, 2011) and thin-walled channel sections with intermediate web stiffeners (Pham and Hancock, 2009b) in pure shear . These studies provided an effective tool to determine the shear buckling stress which was used to develop the proposed shear design curve in the Direct Strength Method (DSM). However, despite the fact that computational effort is significantly reduced by using the SFSM instead of the Finite Element Method (FEM), SFSM still requires considerable computation. Importantly, the signature curve for shear cannot be isolated. Further, the SFSM analysis assumes no cross-section distortion at both ends of the section under analysis. This restraint at both end sections, therefore, increases the buckling stress above that of the SAFSM where the end sections are free to distort.

The SAFSM provides a simple and sufficient approach to investigate the elastic buckling of thin-walled sections subjected to pure shear. Recently, Hancock and Pham (2011) applied Plank and Wittrick's methodology using complex mathematical techniques and developed a computer program **bfinst7.cpp** employing the SAFSM to study pure shear buckling.

This report is mainly based on **bfinst7.cpp** to investigate the elastic buckling stresses of lipped channel sections with complex web stiffeners in pure shear. Three cases of web stiffeners are considered in this study. They are one rectangular stiffener, one triangular stiffener and two triangular stiffeners in the web. The signature curves and corresponding buckling mode shapes for the different cases are presented and discussed.

MODELLING LIPPED CHANNEL SECTIONS WITH COMPLEX WEB STIFFENERS IN SHEAR

GEOMETRY OF LIPPED CHANNEL SECTIONS WITH COMPLEX WEB STIFFENERS

The geometries of the lipped channel sections with complex web stiffeners are shown in **Fig.1**. It should be noted that the study by Pham and Hancock (2009a, 2011) by using the SFSM proved that varying the flange width has considerable influence on the shear behaviour of a channel section. The elastic shear buckling stress seems to reach a maximum value when the ratio of the flange width to the web depth increases up to 0.4 and slightly reduces for a greater ratio. Therefore, the channel section herein is based on the above optimized ratio which consists a 200mm web depth, 80mm flange width, 20mm lip size and all with thickness 2mm. The stiffeners are located symmetrically about the centre of the web.

Three cases of a lipped channel section with complex web stiffeners include one rectangular stiffener (called **Case A**), one triangular stiffener (called **Case B**), and two triangular stiffeners (called **Case C**). In **Case A**, the variables are the indent (b_{s2}) varying from 5mm to 50mm and the stiffener depth (b_{s1}) varying from 5mm to 190mm. In **Case B**, the angle of the stiffener inclined portions is 45° relative to the horizontal direction and its overall depth (d_s) varies from 5mm to 100mm. While the stiffener shapes and variables for **Case C** are similar to those in **Case B**, the location of each stiffener in **Case C** is at the centre of each half of the web.

The sections are subdivided into longitudinal strips. In all cases, the number of strips in each flange and lip are 4 and 2 respectively. For the strips in the flat portions of the web, both **Cases A&B** have 8 equal strips while **Case C** has 14 strips. The stiffener depth is divided into 6 equal strips and the indents into 2 each in **Case A** while each of the inclined portions is divided into 4 equal strips in both **Cases B&C**.

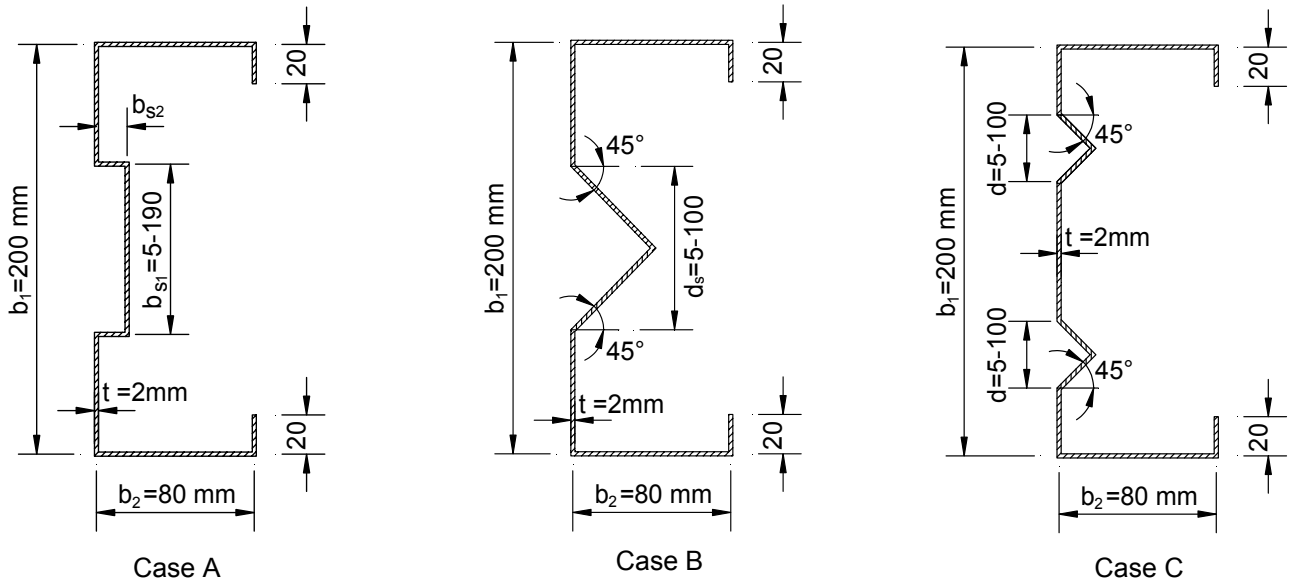

Figure 1. Lip Channel Geometry with Intermediate Stiffeners

SHEAR FLOW DISTRIBUTION

The shear flow distribution resulting from a shear force parallel with the web and acting through the section shear centre is shown in **Fig. 2**. In order to simulate the variation in shear stress, each strip in the cross-section is assumed to be subjected to a pure shear stress which varies from one strip to the other. The more the cross-section is subdivided into strips, the more accurately the shear stress is represented in order to match the practical shear flow distribution.

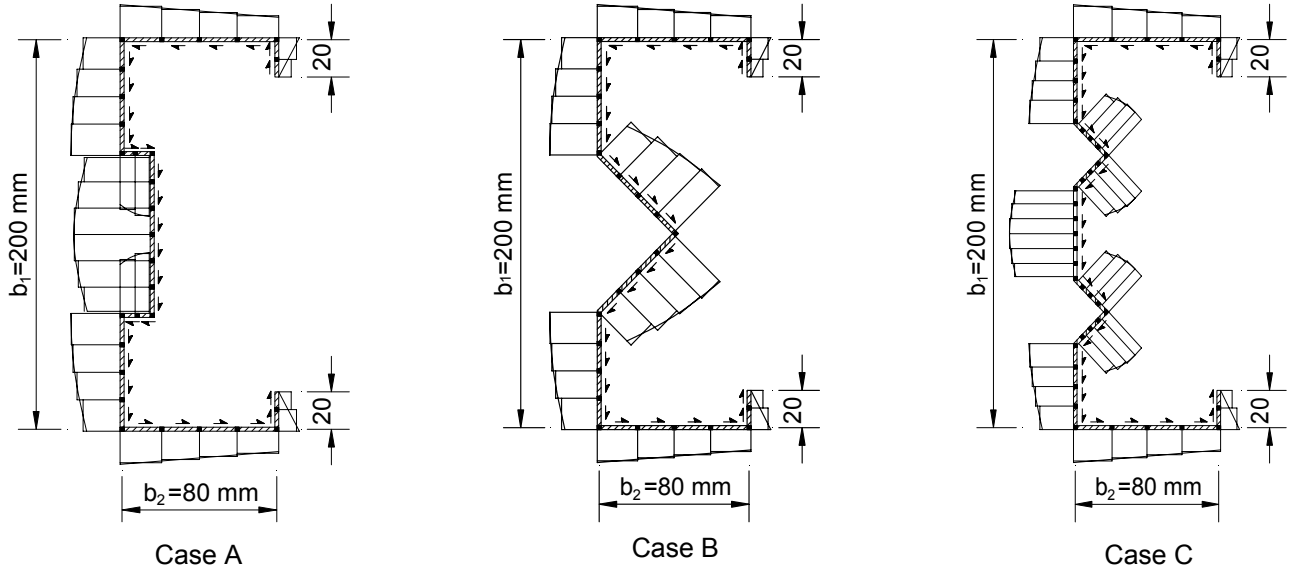

Figure 2. Shear Flow Distribution

RESULTS OF BUCKLING ANALYSES

ELASTIC SHEAR BUCKLING OF CHANNEL SECTION WITH ONE RECTANGULAR WEB STIFFENER (CASE A)

Fig. 3 shows the shear buckling stress versus half-wavelength curves (signature curves) for **Case A** when b_{s2}=5mm and b_{s1} varies from 5mm to 190mm. **Fig. 4** graphically displays several buckling mode shapes at the half-wavelength corresponding to minimum stress or at a similar half-wavelength when a minimum point does not exist.

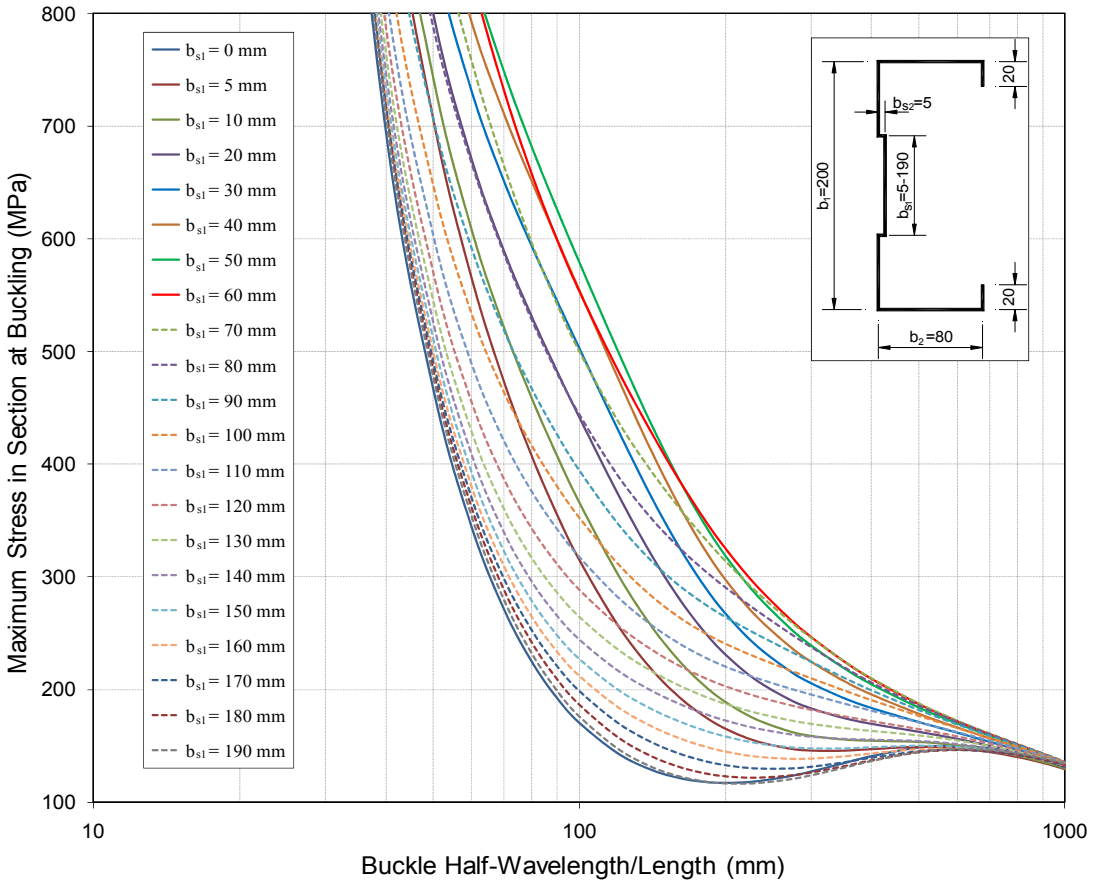

Figure 3. Signature Curves for Case A (b_{s2}=5mm)

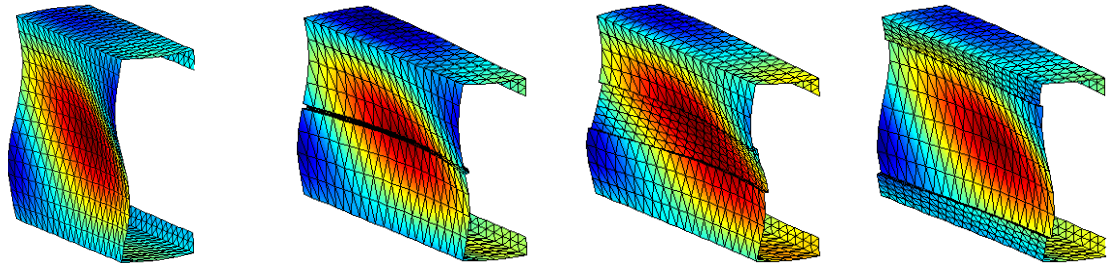

(a) b_{s1}=0, HWL 200mm*

(b) b_{s1}=5mm, HWL=350mm*

(c) b_{s1}=50mm, HWL=350mm

(d) b_{s1}=150mm, HWL=350mm*

*Note: * denotes the half-wavelength where the minimum point exists.*

Figure 4. Buckling Mode Shape for Case A (b_{s2}=5mm)

It is evident that when the stiffener is very small (b_{s1} =5mm, b_{s2} =5mm), a minimum exists and the member buckles locally in the whole web at the half-wave length of 350mm as shown in **Fig. 4b**. Clearly, this is not pure local buckling since the junction lines between the web and the stiffener distort. It is worth noting that for a plain channel section in pure shear, local buckling as can be seen in **Fig. 4a** occurs at a half-wavelength equal to the section depth (200mm). Interestingly, with the presence of even a very small stiffener, the buckling half-wavelength corresponding to the minimum point has significantly been lengthened up to 350mm. Also, the shear buckling stress is considerably improved by 24.4% compared to that of a plain channel section.

As can be seen in **Fig. 3,** when the stiffener depth (b_{s1}) increases further, the minimum point is completely removed from the signature curve. In the web, the buckling mode gradually changes from the whole web to the stiffener depth (b_{s1}). At the stiffener depth (b_{s1}) of 60mm where the web is approximately divided into three equal vertical flat portions, the shear buckling stress seems to reach the maximum value. When the stiffener depth increases further, the signature curve starts dropping to approach that of the plain channel

section. At b_{s1}=150mm, the minimum point reappears at the half-wavelength of 350mm and the shear buckling stress of 147.9 MPa which is not much different from the buckling stress of the section with the very small stiffener as described previously (145.9 MPa).

As shown in **Fig. 5** where signature curves are plotted for the case of b_{s2}=10mm and variable b_{s1} (from 5mm to 190mm), when the stiffener width (b_{s2}) increases to 10mm, although the stiffener depth may be very small (b_{s1}=5mm), the minimum is completely eliminated and only appears when b_{s1}=170mm. The signature curve is shifted up continuously when b_{s1} increases from 5 mm and lies on the highest position at b_{s1}=60mm where the shear buckling stress seems to have a maximum value. For greater stiffener depths (b_{s1}>60mm), the curve starts dropping and forms the minimum at b_{s1}=170mm. By comparison with the case of b_{s2}=5mm, the shear buckling stress are significantly improved for the wider stiffener (b_{s2}=10mm). For instance, the shear buckling stresses of the section are 145.9MPa and 192.5MPa for b_{s2}=5mm and b_{s2}=10mm, respectively with the same b_{s1}=5mm and at the half-wavelength of 350mm.

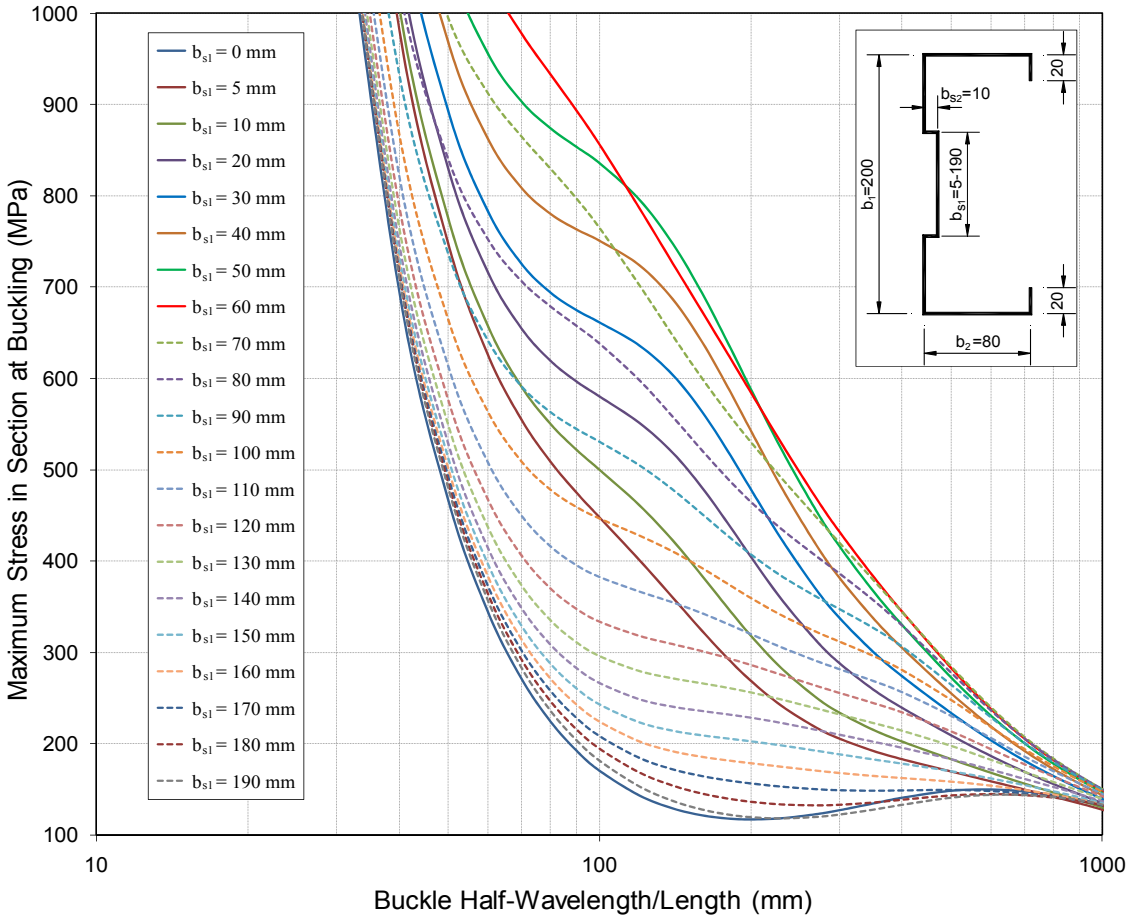

Figure 5. Signature Curves for Case A (b_{s2}=10mm)

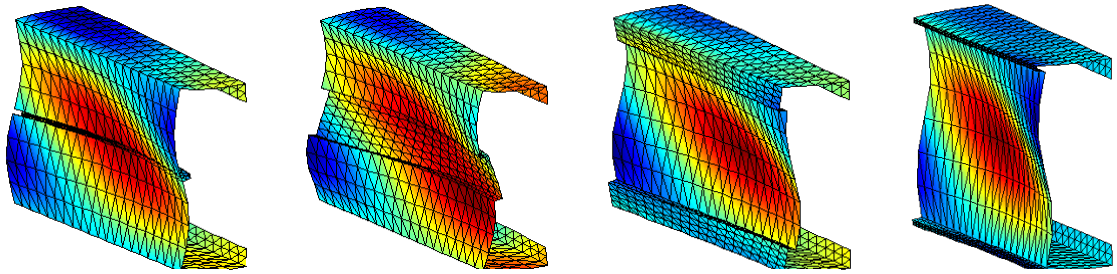

(a) b_{s1}=5mm, HWL=350mm

(b) b_{s1}=50mm, HWL=350mm

(c) b_{s1}=150mm, HWL=350mm

(d) b_{s1}=190mm, HWL=230mm*

Figure 6. Buckling Mode Shape for Case A (b_{s2}=10mm)

The buckling mode shapes for b_{s2}=10mm as shown in **Fig. 6** are similar to those for b_{s2}=5mm. When the stiffener depth (b_{s1}) is small, the buckle occurs mainly in the whole web and gradually concentrates to the stiffener depth. At smaller half-wavelengths, the section is buckled in the flat portions of the web and the buckling mode spreads to the whole web at the longer half-wavelengths.

For the case of b_{s2}=15mm and variable b_{s1} (from 5mm to 190mm) as shown in **Fig. 7**, the shear signature curves are very interesting. When b_{s1} increases from 5mm to 20mm, the shear buckling stress of the section is clearly enhanced and a minimum point does not exist. At larger stiffener depth (b_{s1}), the occurrence of the minima does not follow the regular tendency as can be seen in previous cases. In order to provide an overview, the summary of the buckling analyses is given in **Table 1** and specifies when the minima of the signature curves form with the corresponding shear buckling stresses and buckling half-wavelengths.

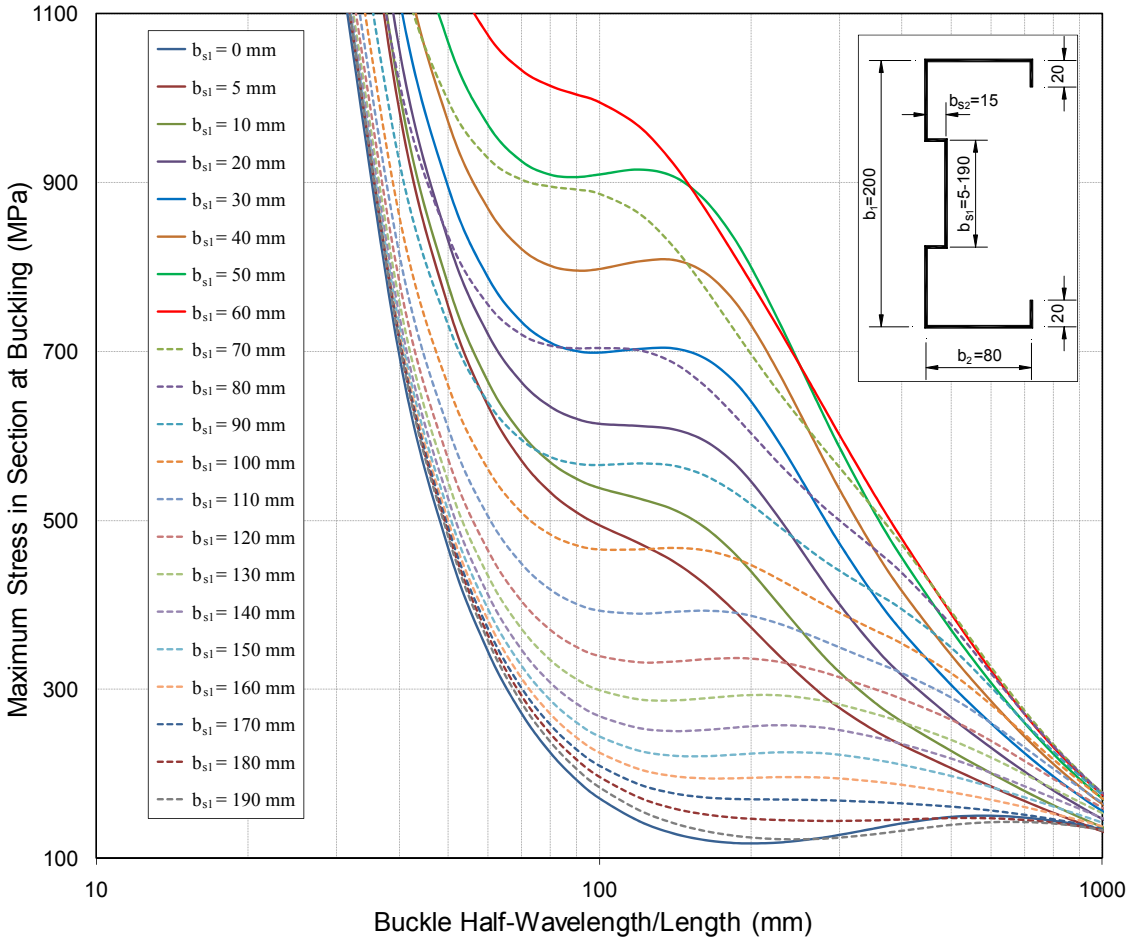

Figure 7. Signature Curves for Case A (b_{s2}=15mm)

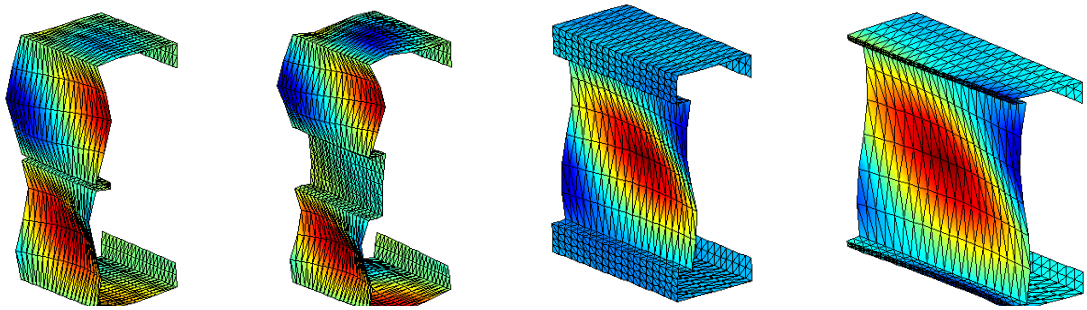

(a) b_{s1}=5mm, HWL=90mm

(b) b_{s1}=50mm, HWL=90mm*

(c) b_{s1}=150mm, HWL=160mm*

(d) b_{s1}=190mm, HWL=230mm*

Figure 8. Buckling Mode Shape for Case A (b_{s2}=15mm)

As indicated in **Table 1** and previous figures, for the small stiffener widths (b_{s2}=5mm, b_{s2}=10mm), the local buckling stresses in shear are significantly improved. A minimum point only appears when either the stiffener is very small (b_{s1}=b_{s2}=5mm) or the stiffener depth is very large (b_{s1}≥150mm for b_{s2}=5mm and b_{s2}≥170mm for b_{s2}=10mm). At b_{s2}=15mm, the minima are more commonly formed and they are almost always available when b_{s2} reaches the magnitude of 20mm. When b_{s2} increases further, a minimum is always determined irrespective of the stiffener depth (b_{s1}). However, the shear buckling stress enhancement tends to decrease from the maximum value achieved at b_{s2}=20mm. The explanation is mainly based on the very high slenderness of the stiffener width.

Table 1: The Summary of Buckling Stresses and Corresponding Buckling Half-wavelengths

b_{s1}(mm)	b_{s2} (mm)						
	5	10	15	20	30	40	50
5	145.915 (350)	-	-	-	513.803 (100)	512.623 (100)	506.867 (100)
10	-	-	-	546.373 (120)	551.370 (100)	548.631 (100)	542.449 (100)
20	-	-	-	620.824 (100)	620.214 (90)	614.662 (90)	608.697 (90)
30	-	-	698.933 (100)	702.404 (90)	698.957 (90)	692.610 (90)	685.443 (90)
40	-	-	795.999 (90)	799.068 (90)	795.674 (90)	788.701 (90)	779.764 (90)
50	-	-	906.704 (90)	911.955 (80)	908.431 (80)	901.577 (80)	890.834 (80)
60	-	-	-	1031.243 (80)	1033.134 (80)	1022.418 (80)	994.860 (80)
70	-	-	-	900.328 (70)	874.810 (70)	847.067 (70)	818.298 (80)
80	-	-	703.926 (90)	702.998 (80)	681.664 (80)	659.947 (80)	639.972 (80)
90	-	-	565.642 (100)	563.982 (90)	546.771 (90)	529.275 (90)	513.896 (90)
100	-	-	465.707 (100)	463.295 (100)	449.369 (100)	435.053 (100)	422.704 (100)
110	-	-	389.460 (120)	389.275 (100)	377.505 (100)	366.284 (100)	356.865 (100)
120	-	-	331.932 (120)	330.597 (120)	321.519 (120)	311.694 (120)	303.229 (120)
130	-	-	286.775 (140)	285.655 (120)	277.878 (120)	270.050 (120)	263.389 (120)
140	-	-	250.422 (140)	249.661 (140)	243.820 (140)	237.039 (140)	263.389 (120)
150	147.902 (350)	-	220.515 (160)	219.996 (140)	215.187 (140)	209.797 (140)	205.117 (140)
160	138.688 (270)	-	194.284 (180)	194.919 (160)	192.206 (160)	188.038 (160)	184.075 (160)
170	129.994 (270)	148.622 (350)	-	172.372 (180)	171.424 (160)	168.650 (160)	165.841 (160)
180	121.831 (230)	132.568 (270)	143.832 (300)	150.324 (200)	152.247 (180)	151.300 (180)	149.780 (180)
190	116.765 (200)	118.265 (230)	122.195 (230)	125.632 (270)	131.997 (230)	133.530 (200)	133.764 (200)

- Note: In each cell, the first number is the buckling stress (MPa) corresponding to a minimum and the number in the brackets is the corresponding buckling half-wavelength (mm).

Attention is turned to the case of b_{s2}=15mm where some notable transitions occur as can be seen in **Fig. 7** and **Fig. 9**. As long as the stiffener depth is relatively small (b_{s1} is from 5mm to 20mm), the shear buckling enhancement effect of the stiffener removes the minima from the signature curves. When the stiffener depth (b_{s1}) increases from 30mm to 50mm, the stiffener is stiff enough to separate the web into three vertical flat portions and also acts as a restraint to the upper and lower flat plates to allow those plates and the flanges to buckle locally. However, this is not pure local buckling since there is a slight distortional deformation at the stiffener. It is interesting that the minima can be determined in these cases. At the stiffener depths of 60mm and 70mm, the stiffener is slender enough to allow local buckling to occur simultaneously in the three vertical flat portions. Nevertheless, these buckling modes prevent the presence of a minimum point. As the stiffener becomes deeper (b_{s1} increases further), the shear local buckling mainly locates in the stiffener depth as shown in **Fig. 8d** and the minima reappear. However, no pure local buckling is observed.

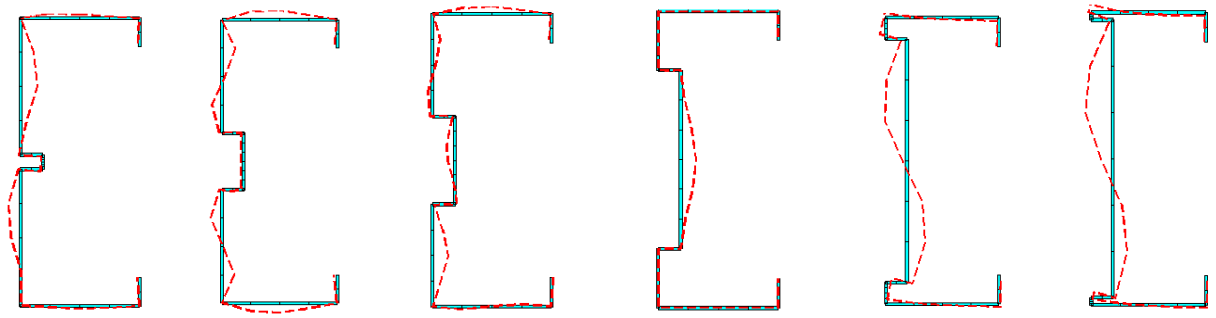

(a) b_{s1}=10mm (b) b_{s1}=40mm (c) b_{s1}=60mm (d) b_{s1}=120mm (e) b_{s1}=170mm (f) b_{s1}=190mm

Figure 9. In-plane Buckling Mode Shape for Case A (b_{s2}=15mm)

It is interesting to note that when b_{s1} increases to 170mm as shown in **Fig. 9**, the minimum point suddenly disappears as shown in **Table 1** and the buckling mode switches from local buckling to distortional buckling. Apparently, small distortional deformations have a significant effect on the buckling behaviour of a channel section with web stiffeners. In this specific study, the occurrence of small distortional deformations at the stiffener widths (b_{s2}) attached to the small vertical components of the web causes the disappearance of the minima. However, more significant distortional deformation (as happens for b_{s1}=180mm, 190mm) does not remove the minima but lengthens the buckling half-wavelengths.

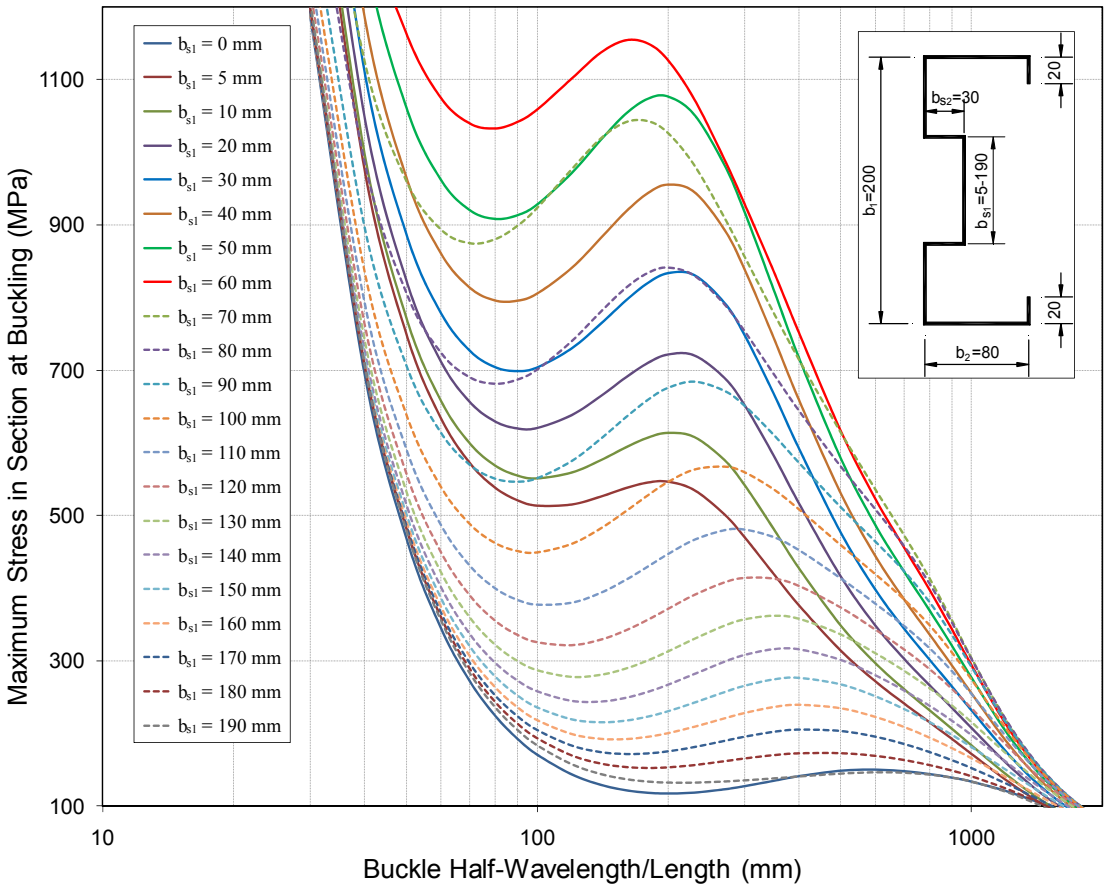

Figure 10. Signature Curves for Case A (b_{s2}=30mm)

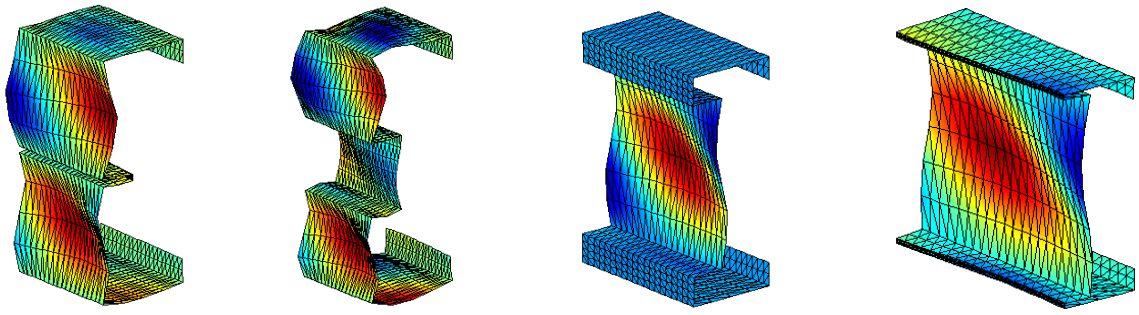

(a) b_{s1}=5mm, HWL=100mm*

(b) b_{s1}=60mm, HWL=80mm*

(c) b_{s1}=150mm, HWL=140mm*

(d) b_{s1}=190mm, HWL=230mm*

Figure 11. Buckling Mode Shape for Case A (b_{s2}=30mm)

For a stiffener width (b_{s2}) of 30mm as shown in **Fig. 10**, the minima always exist irrespective of the dimensions of the stiffener. This is due to the fact that the stiffener width is sufficiently wide to provide restraints to the vertical flat plates and allow local shear buckling to occur mainly either in the flat portions of the web or in the stiffener depth.

The specific buckling mode shape depends on the depth of the stiffener. As long as b_{s1} is relatively small (b_{s1} is less than 50mm), local buckling in the two vertical flat portions of the web governs the shear behaviour of the sections. However, small distortional deformations in the stiffener are also involved. When b_{s1} increases from 50mm to 160mm, pure local buckling exists in which all junction lines remain straight. However, for a larger stiffener depth (b_{s1} is greater than 160mm), distortional deformation reappears in the parts formed by the stiffener widths and the vertical components of the web as can be seen in **Fig. 11d**.

The buckling half-wavelength corresponding to the minimum elastic shear buckling stress is approximately equal to the largest depth among the three vertical flat portion dimensions of the web. This is different from the cases of a small stiffener width (b_{s2}=5mm, b_{s2}=10mm) where the buckling half-wavelengths are always larger than the section depth. The explanation of this difference is mainly due to the increased restraint effect of the larger horizontal components of the rectangular stiffener attached to the small vertical components of the web.

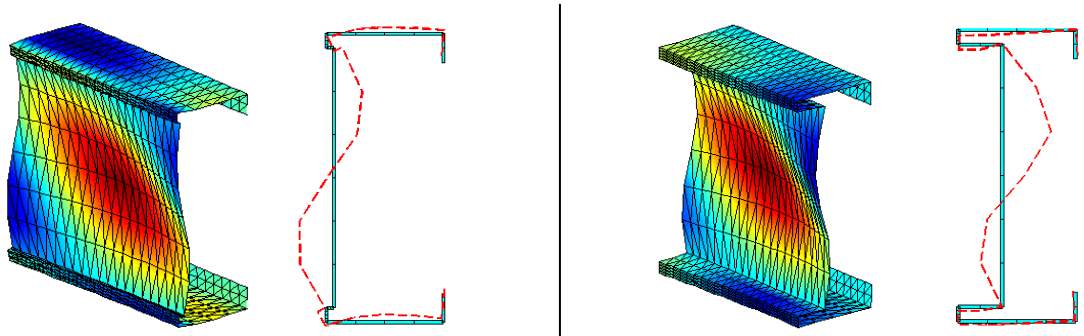

(a) b_{s2}=5mm, HWL 230mm*, Shear buckling stress 121.831MPa

(b) b_{s2}=30mm, HWL 180mm*, Shear buckling stress 152.247MPa

Figure 12. Buckling Mode Shape for b_{s1}=180mm

As shown in **Fig. 12a,** the small stiffener widths (b_{s2}=5mm) attached to the small vertical components of the web are less stiff and so they subsequently buckle with the web. Therefore, the consequent flange deformation is considerable which even leads to a slight distortional deformation of the lip-flange junction. By comparison, when b_{s2} is sufficiently large (30mm) as shown in **Fig. 12b**, the horizontal stiffener components attached to the small vertical web components are torsionally stiffer to adequately provide restraint to the stiffener depth. Thus, the local buckling is allowed to occur mainly in the stiffener depth at a greater shear buckling stress. With b_{s2}=30mm, no distortional deformation in the lip-flange junctions is observed which explains the reason for the fact that the buckling half-wavelengths are smaller to those for b_{s2}=5mm and b_{s2}=10mm.

ELASTIC SHEAR BUCKLING OF CHANNEL SECTION WITH ONE TRIANGULAR WEB STIFFENER (CASE B)

Fig. 13 shows the shear signature curves for **Case B** where the stiffener size is varied. The angle between the inclined web portions and the horizontal direction is unchanged at 45°. When the stiffener is small (d_s=5mm), the buckling mode shape shown in **Fig. 14a** and the buckling stress shown in **Fig. 13** are not significantly different from those of a plain channel section. As d_s increases from 15mm to 40mm, the minimum disappears while the shear buckling stress continues to improve. The signature curve regains the minimum point when d_s is 45mm. As d_s keep increasing to 75mm, the elastic shear buckling stress reaches a maximum value of 1118.2 MPa. For larger stiffeners (d_s is more than 75mm), shear buckling stresses start dropping with a significantly greater increment compared with the increasing increment.

It is evident from **Fig. 14** that the buckling mode gradually relocates from the whole web to the two vertical web flat portions and then spreads to all portions of the web including the inclined ones. When d_s is sufficiently large, the member mainly buckles in the inclined portions of the web. These transitions depend on the slenderness of the stiffener. Pure local buckling only occurs when d_s reaches a magnitude of 55mm.
Similar to the lipped channel section with a small square stiffener (b_{s1}=b_{s2}=5mm) in **Case A**, the lipped channel section with a small triangular stiffener (d_s=5mm) mainly buckles locally in the whole web and also includes a little distortional deformation in the flanges which leads to the fact that the buckling half-wavelength corresponding to the minimum shear buckling stress (230mm) is larger than the section depth (200mm).

Interestingly, a small triangular stiffener (d_s=5mm) only improves the shear buckling stress by 3% which is much smaller than the enhancement of 24.4% for a small square stiffener (b_{s1}=b_{s2}=5mm) in **Case A**.

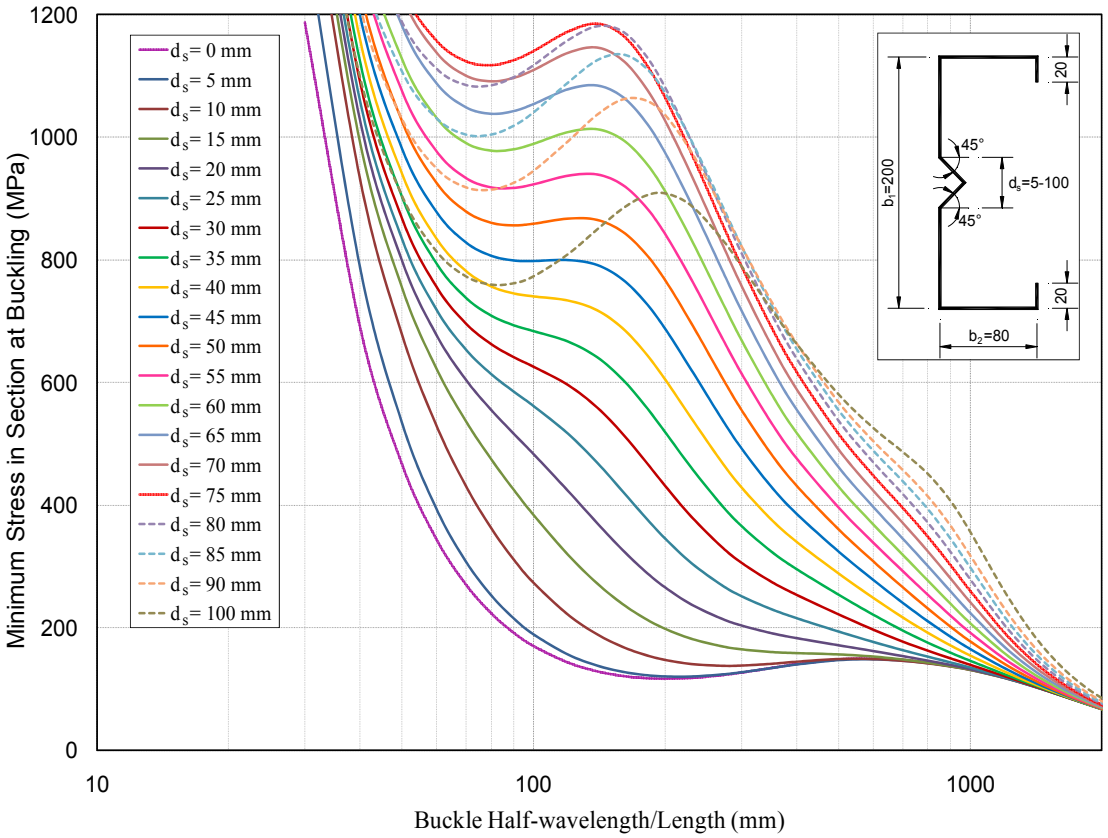

Figure 13. Signature Curves for Case B

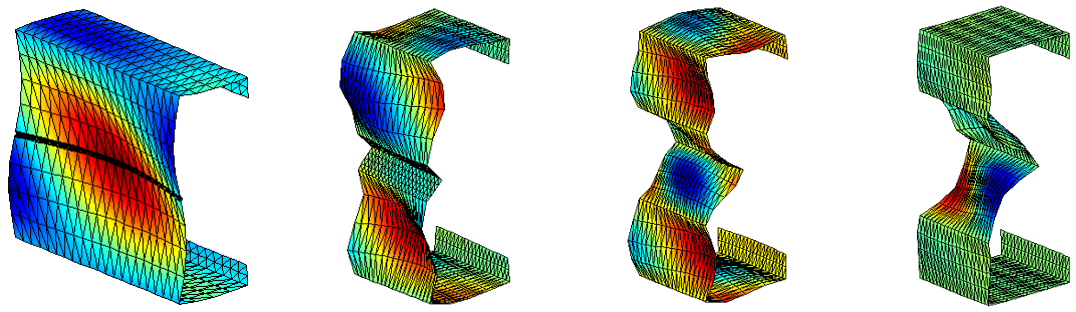

(a) d_s=5mm, HWL=230mm*

(b) d_s =30mm, HWL=90mm

(c) d_s =75mm, HWL=80mm*

(d) d_s =100mm, HWL=80mm*

Figure 14. Buckling Mode Shape for Case B

ELASTIC SHEAR BUCKLING OF CHANNEL SECTION WITH TWO TRIANGULAR WEB STIFFENERS (CASE C)

Fig. 15 and **Fig. 16** show the shear signature curves and corresponding buckling mode shapes of lipped channel section with two triangular stiffeners (**Case C**) respectively. It can easily be seen in **Fig.15** that the presence of two small triangular stiffeners (d_s=5mm) does not significantly improve the shear buckling stresses of the whole section. The section is buckled locally at a half-wave length of 230mm and shear buckling stress is approximately equal to that of a plain channel section. Even when d_s is 10mm, only a 14% improvement is observed.

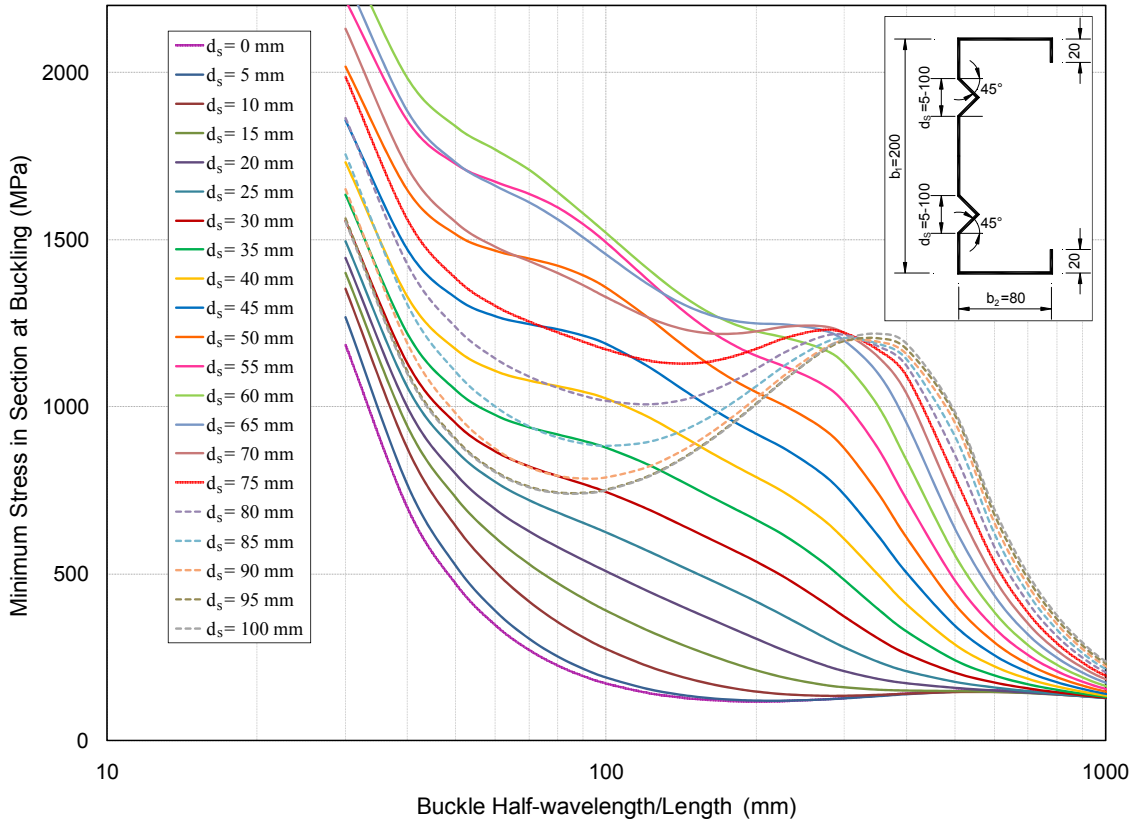

Figure 15. Signature Curves for Case C

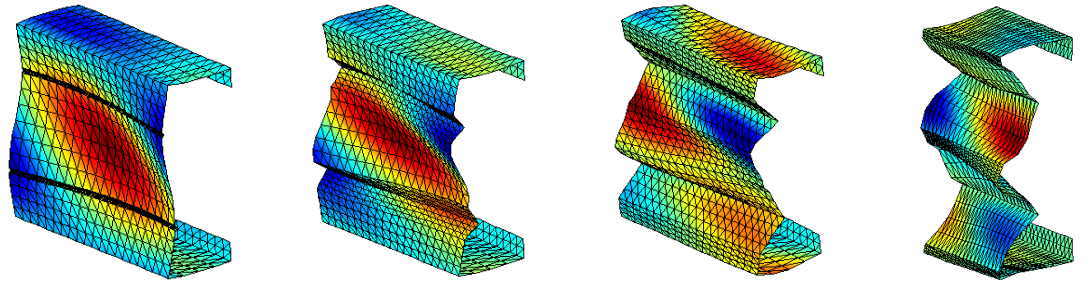

(a) d_s=5mm, HWL=230mm*

(b) d_s=30mm, HWL=200mm

(c) d_s =60mm, HWL=200mm

(d) d_s =85mm, HWL=100mm*

Figure 16. Buckling Mode Shape for Case C

As d_s increases from 15mm to 65mm, the signature curve is shifted up. Consequently, the shear buckling stress is enhanced. In this range of d_s (15mm to 65mm), a minimum point cannot be determined. When d_s increases further from 70mm, the signature curves, with the occurrence of the minima, start dropping at shorter half-wavelengths (up to 300mm) but keep rising at longer half-wavelengths (longer than 300mm). This fact is similar to that of **Case B** (one triangular stiffener) which shows that distortional stress is always improved by adding triangular stiffener(s).

CONCLUSION

The shear signature curves and buckling mode shapes of channel sections with three types of web stiffeners in pure shear are studied by means of the **bfinst7.cpp** program based on the Semi-Analytical Finite Strip Method (SAFSM). The outcomes prove that the presence of web stiffeners mainly improves the shear buckling stress of sections by increasing the local buckling stress. In all cases, the web stiffeners have only a minor effect on improving the distortional buckling stress.

For rectangular stiffeners, a minimum tends to exist for either the thin and deep stiffener (small b_{s2} and large b_{s1}) or wide stiffener (large b_{s2}). For triangular stiffeners, minimum points occur if the stiffeners are very small or large enough. Pure local buckling in shear (all line junctions remain straight) seem to have the minimum points and they only occur when the stiffeners are sufficiently large to allow local buckling in each flat portion.

Distortional buckling in the web in shear occurs when the line junctions do not remain straight and generally do not have minima. However, minima may occur in the following three cases: (1) the stiffeners are very small where it is essentially a local buckle of the whole web stiffened slightly by the small stiffeners (orthotropic plate), (2) the stiffener depth (b_{s1}) of the rectangular stiffener is very large where the horizontal stiffener components attached to the very small vertical web components act to reduce the influence of the distortional mode, or (3) the stiffener width (b_{s2}) of the rectangular stiffener is large enough to provide restraints to the web plates where local buckling mainly occurs.

The incorporation of slight distortional deformation in the mode where the minimum point exists leads to the lengthening of the corresponding buckling half-wavelength.

It seems that with approximately the same amount of steel, the lipped channel section with a rectangular stiffener is more effective than that of a triangular stiffener in shear in terms of the shear buckling stress. For all lipped channel sections with different web stiffeners, shear buckling stress reaches a maximum value when the web is subdivided into approximately equal flat portions which are formed by the stiffeners.

ACKNOWLEDGEMENT

Funding provided by the Australian Research Council Discovery Project Grant DP110103948 has been used to perform this project.

REFERENCES

Allen, H. G and Bulson, P., Background to Buckling, McGraw-Hill Book, 1980.

American Iron and Steel Institute (AISI). (2007). "North American Specification for the Design of Cold-Formed Steel Structural Members." 2007 Edition, AISI S100-2007.

Cheung, Y.K. (1976), Finite Strip Method in Structural Analysis, Pergamon Press, Inc. New York, N.Y.

Hancock, G. J. and Pham, C. H. (2011). "A Signature Curve for Cold-Formed Channel Sections in Pure Shear", Research Report R919, The University of Sydney, July.

Hancock, G. J. (1978), "Local, Distortional and Lateral Buckling of I-Beams", Journal of the Structural Division, ASCE, Vol. 104, No. ST11, pp 1787-1798.

Lau, S. C. W. and Hancock, G. J. (1986), "Buckling of Thin Flat-Walled Structures by a Spline Finite Strip Method." Thin-Walled Structures, Vol. 4, pp 269-294.

Pham, C. H. and Hancock, G. J. (2009a). "Shear Buckling of Thin-Walled Channel Sections." Journal of Constructional Steel Research, Vol. 65, No. 3, pp. 578-585.

Pham, C. H. and Hancock, G. J. (2009b). "Shear Buckling of Thin-Walled Channel Sections with Intermediate Web Stiffener." Proceedings, Sixth International Conference on Advances in Steel Structures, Hong Kong, pp. 417-424.

Pham, C. H. and Hancock, G. J. (2011). "Elastic Buckling of Cold-Formed Channel Sections in Shear." Proceedings, International Conference on Thin-Walled Structures, Timisoara, Romania, pp 205-212, Volume 1.

Plank, R. J., and Wittrick, W. H. (1974), "Buckling Under Combined Loading of Thin, Flat-Walled Structures by a Complex Finite Strip Method", International Journal for Numerical Methods in Engineering, Vol. 8, No. 2, pp 323-329.

Przmieniecki, J. S .D. (1973), "Finite Element Structural Analysis of Local Instability", Journal of the American Institute of Aeronautics and Astronautics, Vol. 11, No. 1.

Standards Australia. (2005). "AS/NZS 4600:2005, Cold-formed Steel Structures." Standards Australia/ Standards New Zealand.